6-2021

Impact of New Generation Wide-Base Tires on Fuel Consumption

Izak M. Said
University of Illinois - Urbana-Champaign

Egemen Okte
University of Illinois - Urbana-Champaign

Jaime Hernandez
Marquette University, jaime.hernandez@marquette.edu

Imad L. Al-Qadi
University of Illinois - Urbana-Champaign

Journal of Transportation Engineering, Part B: Pavements, Vol. 147, No. 2 (June 2021): 04021011. DOI.

Impact of New Generation Wide-Base Tires on Fuel Consumption

Izak Said
Department of Civil and Environmental Engineering, University of Illinois at Urbana-Champaign, Urbana, IL
Egemen Okte
Department of Civil and Environmental Engineering, University of Illinois at Urbana-Champaign, Urbana, IL
Jaime Hernandez
Department of Civil and Environmental Engineering, Marquette University, Milwaukee, WI
Imad L. Al-Qadi
Engineering, Illinois Center for Transportation, University of Illinois at Urbana-Champaign, Urbana, IL

Abstract

This study combined multiple approaches to evaluate the structural and economic impact of using new-generation wide-base tires (NG-WBT) in New Brunswick, Canada. A three-dimensional finite-element model of a typical pavement structure used in New Brunswick was used to predict critical pavement responses. The model includes measured tire-pavement contact forces among other

variables overlooked in conventional flexible pavement analysis approaches. Using the model output, regression analysis was performed to predict the responses under various loadings to avoid performing the time-consuming finite-element analysis. Eight-year weight-in-motion data and critical pavement responses were used in transfer functions to predict pavement damage and the corresponding progression of an international roughness index (IRI) during a 60-year analysis period. Most pavement responses from NG-WBT compared with dual-tire assembly (DTA) were 20% and 30% higher in this case. The smallest difference was the vertical strain on top of the subgrade. The life cycle cost analysis (LCCA) considered a reduction in fuel consumption because of the use of NG-WBTs. Two scenarios were analyzed: (1) Case A, in which maintenance was performed periodically and independent of IRI values, and (2) Case B, in which the IRI threshold triggered maintenance. A reduction in fuel costs was significant in both cases. Maintaining a low pavement IRI would increase vehicle and truck fuel cost savings. The results indicate that the agency cost to maintain pavement used by NG-WBT is expected to be between CAD 7,703 to CAD 8,840 (2019 dollars) for 10% and 20% of all tandem axles using NG-WBT per one kilometer for a 60-year analysis period. The annual worth of such savings would be CAD 298 and CAD 342 (2019 dollars), respectively. In contrast, fuel savings per truck-km is expected to be CAD 30,471 to CAD 60,119 (2019 dollars) for 10% and 20% of all tandem axles using NG-WBT per one kilometer for the same analysis period, respectively. The annual worth of such savings would be CAD 1,100 and CAD 2,172 (2019 dollars) per one kilometer, respectively. Additionally, the trucks would save, annually, CAD 0.42 and CAD 0.107 per ton transported per kilometer for 10% and 20% NG-WBT market penetrations, respectively.

Introduction

Replacing trucks' dual-tire assembly (DTA) with wide-base tires (WBT) is one of the options to reduce the environmental impact in transportation. In addition, WBT is more fuel efficient than DTA because it reduces gross truck weight, requires less frequent replacement, and has relatively lower maintenance costs (Al-Qadi and Elseifi 2007). Despite the benefits, studies in the 1980s and 1990s reported that WBTs caused more pavement damage than DTA. This drawback motivated the tire industry to produce the so-called new-generation WBT (NG-WBT) in the early 2000s. Since then, studies indicated that NG-WBT caused similar (Al-Qadi et al. 2002) or slightly more (Al-Qadi et al. 2017, 2018) damage than DTA, depending on NG-WBT and loaded pavements. However, current pavement structural evaluations exclude NG-WBT's economic benefits, such as fuel efficiency and truck payload. Consequently, a methodology such as life cycle cost analysis (LCCA) may be used to assess the long-term economics of pavement infrastructure subjected to NG-WBT.

The two main pillars of the LCCA are agency and user costs. Agency costs are associated with constructing and rehabilitating the pavement structure during its analysis period. User costs are incurred by the user for traveling on the pavement. These costs are work zone delays, excessive fuel consumption because of the pavement condition, tire and maintenance costs, crash costs, and emission costs. Studies indicated that WBTs could reduce user costs by up to 1.5% per axle and increase the carrying capacity by 1.5% per axle (Kang et al. 2019). At the same time, an increase in pavement roughness because of potential greater pavement damage would increase fuel consumption (Chatti and Zaabar 2012).

The objective of this study is to perform the LCCA to quantify the trade-off between NG-WBT's economic advantages and disadvantages in New Brunswick, Canada. The quantification combined analytical (finite-element method and regression analysis), experimental (measured tire-pavement contact stresses), field [weight-in-motion (WIM) data], and empirical (pavement-damage estimation using transfer functions) tools to assess the economic impacts of NG-WBT market penetration.

Methodology

Fig. 1 summarizes the adopted procedure to perform the LCCA. The procedure combines the finite-element (FE) method, WIM data, regression analysis, pavement-damage calculation, and prediction of the international roughness index (IRI) progression. FE analysis was used to calculate critical pavement responses for four load magnitudes. Based on the FE results, regression analyses were performed to predict critical pavement responses for any axle type (i.e., single, tandem, and tridem) and load magnitude. Pavement damage, which utilizes critical pavement responses as input, was estimated using transfer functions, whereas IRI progression was predicted using the mechanistic-empirical pavement design guide (MEPDG) (AASHTO 2008). These empirical equations provide a simple approach to directly using pavement responses to predict failure. Finally, pavement damage and IRI progression were used in the LCCA to determine the economic impact of using NG-WBT. The following sections provide further details on the main blocks in Fig. 1.

Weight-In-Motion

Weight-in-motion data collected over eight years in New Brunswick was processed following the MEPDG procedure to determine traffic characteristics. The characteristics included average annual daily truck traffic (AADTT), AADTT in the base year, and normalized truck traffic distribution based on FHWA vehicle classes. The average vehicle class distribution was determined by averaging the number of trucks per class for all years with measurements. The analysis also computed the monthly adjustment factor. Finally, the load on each axle allowed the calculation of the normalized axle load spectra, which is presented in Fig. 2. The first column corresponds to a single axle, whereas the second and third columns represent tandem and tridem axles, respectively. Within each class and axle type, the normalized load spectra represent percentages of the axles in each load interval. The traffic characteristics are relevant to determine pavement damage and IRI progression during the analysis period.

Critical Pavement Responses

Finite-element analysis provided the critical pavement response, which is one of the main inputs in damage prediction. The three-dimensional (3D) pavement model includes variables usually overlooked in conventional analyses of flexible pavement, such as dynamic analysis (Yoo and Al-Qadi 2007), moving load (Yoo et al. 2006), linear viscoelastic asphalt concrete (AC), nonlinear granular materials, 3D contact loads (Al-Qadi and Yoo 2007), nonuniform temperature distribution in the AC layer, and interactions between pavement layers (Yoo et al. 2006). Comprehensive details of the FE model may be found elsewhere (Said et al. 2020; Hernandez et al. 2016). Model validation (i.e., comparison between computer predicted and measured pavement responses) was performed in a previous study using the same modeling approach presented in this study (Al-Qadi et al. 2018). Thirty-two cases were considered in the FE model in this study. The cases result from combining four environmental

conditions (wet, dry, spring-thaw, and frozen), four tire loads (27, 36, 44, and 62 kN), and two tire configurations (DTA and NG-WBT).

Finite Element Model Inputs

Four inputs are used in the model: layer configuration, material properties, loading, and environmental conditions. For the layer configuration, the pavement structure used in the analysis is a typical pavement section in New Brunswick, Canada. It is composed of a 140-mm-thick140-mm-thick AC layer, 150-mm-thick150-mm-thick granular base, and 450-mm-thick450-mm-thick subbase on top of a 600-mm600-mm layer of Borrow A material and a glacial till.

Three material models were considered: linear viscoelastic AC, nonlinear stress-dependent granular base material, and linear elastic subgrade. The AC linear viscoelastic's Prony's series terms were determined from the Long-Term Pavement Performance (LTPP) database for New Brunswick. The terms in the Prony series, Eq. (1), were obtained by fitting a generalized Maxwell model to the dynamic modulus in the LTPP. The generalized Maxwell model has the following form:

(1)

$$E(t) = E_\infty + \sum_{n=1}^{N} E_i \exp\left(-\frac{t}{\tau_n}\right)$$

where $E(t)$ = relaxation modulus at time t; E_∞ = residual relaxation modulus; N = number of dashpot-spring elements; E_i = spring constant; and τ_i = relaxation time. Table 1 summarizes the generalized Maxwell coefficients.

Table 1. Prony series coefficients

E_i	τ_i
1,439.24	1.00×10^{-6}
2,803.27	1.00×10^{-5}
3,841.67	0.0001
3,302.01	0.001
4,335.10	0.01
3,208.31	0.1
2,186.80	1
1,103.99	10
398.68	100
252.29	1,000
78.10	10,000

The granular base was modeled as nonlinear stress-dependent, and the constants were obtained from an Illinois Center for Transportation (ICT) database test results (Tutumluer 2009). This material model is appropriate for the relatively thin AC pavement section at hand. Thin AC causes high stresses in the granular base, thus triggering nonlinear behavior. From the database, k-values for the model in Eq. (2) can be determined:

(2)

$$M_r = k_1 p_a \left(\frac{\theta}{p_a}\right)^{k_2} \left(\frac{\tau_{\text{oct}}}{p_a} + 1\right)^{k_3}$$

where M_r = resilient modulus; k_1, k_2, and k_3 = regression coefficients; $\theta = \sigma_1 + \sigma_2 + \sigma_3$ = bulk stresses; $\tau_{\text{oct}} = \sqrt{2}/3(\sigma_1 - \sigma_3)$ = octahedral shear stress; and papa = atmospheric pressure. The k-values, $k_1 = 4{,}272.4$, $k_2 = 0.631$, and $k_3 = -0.134$, were considered for the base layer. Finally, subbase and subgrade were assumed to be linear elastic. The New Brunswick Department of Transportation provided a resilient modulus of 76 MPa and a Poison's ratio of 0.40 for the subbase. The subgrade's resilient modulus is seasonally dependent, and Table 2 presents the values.

Table 2. Resilient modulus of Borrow A and glacial till and corresponding yearly distribution

Moisture condition	M_r (MPa)	Duration (months)	Surface temperature (°C)
Wet	34.5	5	7.0
Dry	44.8	5	17.0
Spring-Thaw	27.6	1	3.3
Frozen	138	1	−8.3

Variations in the subgrade's resilient modulus and temperature profile in the AC accounted for the environmental conditions. Because there is no distinction between the "Borrow A" layer and the underlying "Glacial Till" in New Brunswick, the resilient moduli of these two layers were adjusted to the same values. Table 2 presents the yearly distribution of a subgrade effective resilient modulus. The temperature distribution along the depth of the AC layer was determined using an analytical one-dimensional temperature distribution model for the AC layer (Wang et al. 2009; Hernandez et al. 2016). The surface temperature, a defining factor for the temperature distribution, corresponded to the quarterly average temperature in New Brunswick.

The loading consisted of measured 3D contact forces for DTA (275/80R22.5) and NG-WBT (DTA445/50 R22.5) loaded at 27, 36, 44, and 62 kN, with a tire inflation pressure of 690 kPa (Hernandez et al. 2013). Using experimentally measured contact forces would improve the accuracy of the calculated critical pavement responses, especially those near the pavement surface (Al-Qadi and Yoo 2007).

Critical Pavement Responses—Single Axle

Critical pavement responses are linked to pavement distresses through transfer functions. The critical pavement responses of interest in this study are tensile strain at the bottom of the AC ($\varepsilon_{11,botac}$), vertical strain on top of the subgrade ($\varepsilon_{22,subgrade}$), transverse tensile strain on the surface of the AC ($\varepsilon_{33,topac}$), and vertical shear strain in the AC layer ($\varepsilon_{23,ac}$). Each critical pavement response is linked to distress. Tensile strain at the bottom of the AC is associated with bottom-up fatigue cracking. Vertical shear strain in the AC layer and transverse tensile strain on the AC's surface are related to AC rutting and near-surface fatigue cracking, respectively. Subgrade rutting is highly correlated with the vertical strains on top of the subgrade.

Fig. 3 compares the critical pavement responses for the four environmental conditions and two tires considered at a 36 kN load. NG-WBT generated 9 με higher $\varepsilon_{11,botac}$,botac than DTA. The NG-WBT configuration has a smaller contact area than the DTA (Hernandez et al. 2013), which leads to higher loads at the tire-pavement interface and, hence, greater critical responses, especially near the surface. Concerning the environmental effect, AC temperature was the main factor affecting $\varepsilon_{11,botac}$. Because of AC's viscoelastic nature, its modulus decreases as the temperature increases, thus escalating critical pavement responses. The relatively high contact stresses of NG-WBT would intensify AC layer deformation and, consequently, higher distortion and shear strain. The $\varepsilon_{23,ac}$ from NG-WBT was 3 με higher than those of DTA. The transverse strain at the surface of the AC ($\varepsilon_{33,topac}$) was slightly lower for the NG-WBT configuration than that of DTA. The vertical strain on top of the borrow material and subgrade ($\varepsilon_{22,subgrade}$) were comparable between NG-WBT and DTA. The maximum difference in $\varepsilon_{22,subgrade}$ between tires was 3.6 με. The impact of load distribution diminishes with depth, and after a certain depth, pavement responses are affected mainly by total tire load rather than its distribution on the surface. Similar trends were observed for other considered loads (i.e., 27, 44, and 62 kN).

The results indicated a linear relationship between critical pavement responses and tire load for a specific tire configuration and environmental condition. Table 3 presents the equations that relate load and critical strains with the corresponding coefficients of determination (R^2). The equations are valid for the structure presented in this study, the axle loading between 27 and 62 kN at the corresponding environmental condition, and at a speed of 8 km/h.

Table 3. Linear regression models for critical pavement responses

Moisture condition	Tire	Equation	R^2	Tire	Equation	R^2
Tensile strain at the bottom of AC						
Dry	DTA	$\varepsilon = 1.5154\mathrm{P} + 10.0971$	0.998	NG-WBT	$\varepsilon = 1.6180\mathrm{P} + 18.9998$	0.992
Frozen	$\varepsilon = 0.9281\mathrm{P} + 4.9728$	0.998	$\varepsilon = 0.9859\mathrm{P} + 10.2714$	0.995		
Spring	$\varepsilon = 0.9781\mathrm{P} + 4.8797$	0.998	$\varepsilon = 1.0370\mathrm{P} + 10.1633$	0.995		
Wet	$\varepsilon = 1.0544\mathrm{P} + 5.2495$	0.998	$\varepsilon = 1.1206\mathrm{P} + 10.8307$	0.995		
Vertical shear strain in AC						
Dry	DTA	$\varepsilon = 0.4694\mathrm{P} + 9.5076$	0.998	NG-WBT	$\varepsilon = 0.5455\mathrm{P} + 9.4729$	0.987
Frozen	$\varepsilon = 0.2508\mathrm{P} + 4.9336$	0.998	$\varepsilon = 0.2837\mathrm{P} + 5.7771$	0.998		
Spring	$\varepsilon = 0.2605\mathrm{P} + 4.9123$	0.998	$\varepsilon = 0.2908P + 5.8359$	0.998		
Wet	$\varepsilon = 0.2873P + 5.2745$	0.998	$\varepsilon = 0.3366P + 5.6804$	0.994		
Transverse strain on AC surface						
Dry	DTA	$\varepsilon = 0.3146P - 0.2974$	0.999	NG-WBT	$\varepsilon = 0.3071P - 0.5517$	0.999
Frozen	$\varepsilon = 0.1861P - 0.1032$	0.999	$\varepsilon = 0.1828P - 0.1323$	0.999		
Spring	$\varepsilon = 0.2001P - 0.1632$	0.999	$\varepsilon = 0.1801P + 0.8794$	0.917		
Wet	$\varepsilon = 0.2163P - 0.1689$	0.999	$\varepsilon = 0.2124P - 0.2592$	0.999		
Vertical strain on top of Borrow A						
Dry	DTA	$\varepsilon = -5.4304P + 29.4660$	0.997	NG-WBT	$\varepsilon = -5.2364P + 26.0729$	0.999
Frozen	$\varepsilon = -1.9757P - 7.7804$	0.999	$\varepsilon = -1.9850P - 8.3377$	0.999		
Spring	$\varepsilon = -5.2574P + 23.7073$	0.998	$\varepsilon = -5.2253P + 25.0464$	1.000		
Wet	$\varepsilon = -4.9843P + 25.6326$	0.999	$\varepsilon = -4.8952P + 24.6954$	0.999		

Note: Strains in microstrains and load in kilo-Newtons.

Critical Pavement Responses—Tandem and Tridem Axle

Tandem and tridem axles in the model require a model geometry that significantly increases the already high computational cost. To overcome this limitation, the approach proposed by Fakhri and Ghanizadeh (2014) was extended. In the approach, the variation of critical pavement responses with distance is given as follows in Eq. (3):

(3)

$$Y = \left[\sin\left(\frac{\pi}{2} + \frac{|x|^{\alpha}}{\beta}\right)\right]^{1000}$$

where x = distance from the loading center; Y = normalized stress or strain pulse; and α and β = model parameters that define the shape of the pulse. As presented in Table 3, the parameters α and β were found to vary linearly with tire load, allowing the generation of the strain pulse for any load, even those not included in the FE analysis. The strain pulse was shifted based on tire speed and axle spacing after it was generated. The original and shifted pulses were superposed to determine critical strains for the tandem and tridem axles. A similar procedure was applied to calculate the load duration—relevant in the calculation of AC's dynamic modulus.

Pavement Damage and IRI Progression

Load-related and thermal cracking and rutting define pavement performance and the level of deterioration. The number of repetitions to failure for load-related cracking was calculated using the equation presented in the MEPDG's manual of practice, as follows:

(4)

$$N_f = k_{f1} \times C \times C_H \times \varepsilon^{-k_{f2}} \times E^{-k_{f3}}$$

where N_f = allowable number of applications for load-related cracking; k_{f1}, k_{f2}, and k_{f3} = global field calibration coefficients equal to 0.007566, 3.9492, and 1.281, respectively; E = AC's dynamic modulus in psi; ε_t = critical tensile strain; and C_H = thickness correction term.

The last two terms, ε_t and C_H, depend on the type of cracking. For bottom-up fatigue cracking, the critical strain is the maximum tensile strain at the bottom of the AC, whereas for near-surface cracking, the critical strain is the maximum transverse surface tensile strain. This study also includes another source of near-surface cracking—maximum vertical shear strain in the AC—which usually occurs in the upper 100 mm of the pavement structure (Yoo and Al-Qadi 2008). The thickness correction term for bottom-up ($C_{H,BU}$) and near-surface ($C_{H,NS}$) cracking are calculated as follows:

(5)

$$C_{H,BU} = \frac{1}{0.000398 + \frac{0.003602}{1 + e^{11.02 - 3.49H}}}$$

(6)

$$C_{H,NS} = \frac{1}{0.01 + \frac{12.00}{1 + e^{15.676 - 2.8186H}}}$$

where H = AC's layer thickness in inches. Because the MEPDG rutting procedure requires variations in the vertical strain along the pavement depth, which could not be interpolated from the FE analysis, the Asphalt Institute (AI) equation for rutting is adopted:

(7)

$$N_{f,r} = 1.365 \times 10^{-9} \varepsilon_v^{-4.477}$$

where $N_{f,r}$ = number of load repetitions to reach the allowable rutting (12.5 mm rutting) and ε_v = maximum vertical strain on the subgrade.

The allowable number of repetitions from Eqs. (4)–(7) and traffic information were used to calculate the damage index for each distress and various market penetrations of NG-WBT:

(8)

$$DI = (1 - MP)\frac{n}{N_{f,dta}} + MP\frac{n}{N_{f,wbt}}$$

where DI = damage index; MP = NG-WBT market penetration; n = load applications obtained from a traffic analysis; and $N_{f,dta}$ and $N_{f,wbt}$ = allowable number of load repetitions for DTA and NG-WBT, respectively. The area of the alligator cracking (FC_{BU}) and the length of the surface cracks (FC_{TD}) are given by the following equations, respectively:

(9)

$$FC_{BU} = \frac{1}{60}\frac{C_4}{1 + e^{C_1 \times C_1^* + C_2 \times C_2^* \log(100 DI_{BU})}}$$

(10)

$$FC_{TD} = 10.56\frac{C_8}{1 + e^{C_5 - C_6 \log(DI_{TD})}}$$

where DI_{BU} = damage index for bottom-up cracking; C_1, C_2, and C_4 = transfer regression constants equal to 1.00, 1.00, and 6,000, respectively; DI_{TD} = damage index for near-surface cracking; and C_5, C_6, and C_8 = transfer regression constants equal to 7.00, 3.5, and 1,000, respectively. Rut depth was obtained by multiplying the rutting damage index by the allowable rut depth (12.5 mm).

Thermal cracking is a function of the pavement structure, climate condition, and AC mix properties. Thermal cracking was obtained using AASHTOWare version 2.6.0 Pavement ME Design software. The results are given in Fig. 4.

Once the cracking and rutting are calculated, the IRI progression was calculated:

(11)

$$IRI = IRI_o + 40 \times RD + 0.40 \times FC_{total} + 0.008 \times FC_{thermal}$$

where IRI_o = initial IRI (63.6 in./mi); RD = rut depth (in.); and FC_{total} = combined area of load-related cracking. The number of single, tandem, and tridem axles in each load interval of the load spectra was calculated for a given month. Subsequently, critical pavement responses were computed using the equations derived in the regression analysis, which were replaced in Eqs. (4)–(11) to obtain the cumulative IRI. The final IRI of a given month becomes the initial IRI for the next month, and the procedure is repeated for the entire analysis period.

Life-Cycle Cost Analysis

To perform the analysis, the following assumptions were made.

- The road has two lanes in each direction. The traffic is equally distributed in these directions. The lane width is 3.6 m. Calculations were performed for one direction.
- The pavement length used in the analysis is 1.6 km.
- Based on WIM data, the daily truck traffic is 1,603 vehicles, which is distributed between truck classes, as indicated in Table 4. The table also presents the average tandem axles in a given class. A 1% increase in traffic was assumed for vehicles.
- The 10 truck classes were further classified as medium (classes 4–8) or large trucks (classes 9–13), as defined by HDM-4 (Kerali et al. 2000). This further classification was used to estimate roughness-related fuel consumption (Ziyadi et al. 2018).
- Fuel consumption of NG-WBT is 1.5% less per axle than DTA. Using the information in Table 5, at 100% NG-WBT market penetration (i.e., all tandem axles are equipped with NG-WBT), fuel savings are 0.85% and 4.75% for medium and large trucks, respectively.
- Hauling capacity when using NG-WBT is increased by 1.5% per axle because NG-WBTs are lighter than DTAs. Consequently, for 100% market penetration, the carrying capacity of each truck would increase by 1.71%. Note that this increase in capacity was not included in the fuel cost computations.
- Additionally, the life cycle costs were computed using the methodology explained in Okte et al. (2019) for both agency and fuel costs.
- The price for unit mill and overlay in New Brunswick was set as USD 105 or CDN 136 per metric ton (Holt et al. 2011).
- The analysis period is 60 years with a 1% yearly increase in truck traffic. Therefore, more than 60 years, 30.6 million truck-km are expected for a 1-km1-km section.
- The traffic is composed of 10% trucks and 90% passenger vehicles.
- The discount rate was assumed to be 3% for the analysis period.
- Five market penetrations of tandem axles with NG-WBT were considered: 0% (no tandem axles with NG-WBT), 5%, 20%, 50%, and 100% (all tandem axles with NG-WBT). No NG-WBT was considered in single and tridem axles.
- After each construction/rehabilitation activity, the IRI of the pavement section is returned to 1 m/km, including the initial year of the analysis.
- The unit cost values for the pay items and fuel were obtained from the life cycle inventory database developed at ICT (Al-Qadi et al. 2015). Although values may differ in New Brunswick, the LCCA is comparative in nature, and the trends should hold.

Table 4. Truck distribution and average number of tandem axles per class

Class	Classification	AADTT (%)	Average tandem axles in class	Saving within class (%)	Saving within classification (%)
4	Medium	2.1	0.41	1.23	0.08
5	Medium	22.8	0	0	0.00
6	Medium	4.7	1	3	0.41
7	Medium	0.1	1.55	4.65	0.01
8	Medium	4.4	0.9	2.7	0.35
9	Large	37.0	1.89	5.67	3.18
10	Large	3.3	1.11	3.33	0.17
11	Large	0.1	0.38	1.14	0.00
12	Large	20.0	1.03	3.09	0.94
13	Large	5.5	1.84	5.52	0.46

Table 5. Maintenance schedule of two scenarios

Maintenance activity	Market penetration					
	0%	5%	10%	20%	50%	100%
Case A						
1st	Year 15	Year 15	Year 15	Year 15	Year 15	Year 15
2nd	Year 30	Year 30	Year 30	Year 30	Year 30	Year 30
3rd	Year 45	Year 45	Year 45	Year 45	Year 45	Year 45
4th	Year 60	Year 60	Year 60	Year 60	Year 60	Year 60
5th	—	—	—	—	—	—
Case B						
1st	Year 15	Year 15	Year 15	Year 15	Year 14	Year 13
2nd	Year 27	Year 27	Year 27	Year 27	Year 26	Year 24
3rd	Year 39	Year 39	Year 38	Year 38	Year 37	Year 35
4th	Year 49	Year 49	Year 49	Year 48	Year 47	Year 44
5th	Year 59	Year 59	Year 58	Year 58	Year 56	Year 53

Two cases were considered for the 60-year analysis period, Cases A and B. In Case A, the agency decides to mill the surface and place a 50-mm-thick overlay every 15 years regardless of the pavement condition. Therefore, no threshold set exists for the IRI progression. As a result, the overall IRI is expected to be higher as the market penetration increases. In Case B, the agency sets an IRI threshold of 1.46 m/km, which corresponds to the IRI at 15 years when there is no NG-WBT. Each time the threshold is reached, the agency performs a 50-mm mill and overlay, similar to the previous case. As a result, maintenance planning is expected to change after increasing traffic and NG-WBT market penetration because IRI progression triggers the threshold at various times. Table 5 presents the schedule summary of these cases. Fig. 5 gives the IRI progression plots for different market penetrations. If a maintenance activity has a longer expected life than the time remaining to the end of the analysis period, then the cost of that activity was reduced by the ratio of the remaining analysis time to the expected activity life. For example, if a maintenance activity is performed at the beginning of year 56—five years before the end of the analysis period—and its expected life is 10 years, only 5/105/10 or 50% of its cost is considered in the analysis.

Table 6 summarizes the LCCA results for both cases in Canadian dollars during the year of construction. In Case A, the agency cost does not change with increasing market penetration because of the stringent maintenance schedule. Even though roughness increases with increasing market penetration in both cases, NG-WBT's fuel savings overcome the excessive fuel consumption caused by increased IRI. Because of the low traffic, roughness never reaches levels at which the passenger vehicles are negatively affected in terms of fuel consumption.

Table 6. Present cost in CDN for 2016 year of construction

Cases	Market penetration					
	0%	5%	10%	20%	50%	100%
Case A						
Truck only fuel cost	$6,832,320	$6,818,494	$6,804,669	$6,777,018	$6,694,068	$6,555,815
Truck + PV fuel cost	$21,608,341	$21,595,466	$21,582,595	$21,556,868	$21,479,797	$21,351,697
Agency cost	$361,527	$361,527	$361,527	$361,527	$361,527	$361,527
Difference						
Truck only fuel cost	$0	−$13,826	−$27,651	−$55,302	−$138,252	−$276,504
Truck + PV fuel cost	$0	−$12,875	−$25,746	−$51,473	−$128,544	−$256,644
Agency cost	$0	$0	$0	$0	$0	$0
Case B						
Truck only fuel cost	$6,827,409	$6,813,911	$6,798,975	$6,771,309	$6,688,393	$6,547,625
Truck + PV fuel cost	$21,574,275	$21,563,287	$21,543,114	$21,517,141	$21,439,010	$21,294,150
Agency cost	$417,650	$417,650	$425,353	$426,490	$443,146	$466,410
Difference						
Truck only fuel cost	$0	−$13,498	−$28,434	−$56,100	−$139,016	−$279,784
Truck + PV fuel cost	$0	−$10,988	−$31,161	−$57,134	−$135,265	−$280,125
Agency cost	$0	$0	$7,704	$8,840	$25,497	$48,760

Note: PV = passenger vehicle.

However, savings are still realized for truck and passenger vehicle fuel costs under all scenarios. This trend may change with increased traffic because IRI progresses faster in Case A, and the threshold would be greater with no intervention.

This study's baseline fuel consumption model is based on DTA (Ziyadi et al. 2018). The savings in fuel consumption associated with the use of WBT were deducted from the DTA baseline fuel consumption. Therefore, the LCCA for WBT is directly compared with the LCCA of DTA because the latter is used as a benchmark. Fig. 6 indicates the difference in agency and truck fuel costs for both cases in Canadian dollars at the year of construction. As expected, the overall agency cost for Case A is lower because of the relatively smaller number of maintenance activities. Note that a fuel consumption database created for the United States was used in this study. The exact fuel consumption values may differ slightly for other regions, but the trends remain the same.

From the LCCA, for Case B over an analysis period of 60 years, the agency pays CDN 7,704, CDN 8,840, CDN 25,497, and CDN 48,760 (2019 dollars) extra per kilometer because of the use of NG-WBT at 10%, 20%, 50%, and 100% market penetrations, respectively. In contrast, the trucking industry saves CDN 31,161, CDN 57,134, CDN 135,265, and CDN 128,125 (2019 dollars) in fuel expenses for 10%, 20%, 50%, and 100% market penetrations, respectively, during the same period and pavement section length. For the analysis period of 60 years, 48 million trucks are expected. Therefore, the savings per truck (in CAD) would be 0.06 cents, 0.11 cents, 0.28 cents, and 0.57 cents (2019 dollars) per truck-km for 10%,

20%, 50%, and 100% NG-WBT market penetrations, respectively. Additionally, a metric ton of truck freight costs CDN 12.5 to ship one kilometer in 2019 (Austin 2015). Because the trucks would be able to carry more when using NG-WBT, their shipping cost would be reduced annually by 2.1 cents, 4.2 cents, 10.7 cents, and 21.4 cents (2019 CAD dollars) per truck-km, respectively.

Finally, for passenger vehicles, Case B results in savings because agencies maintain a low overall IRI progression. For passenger vehicles, the annual savings are CDN 2,727, CDN 1,035, CDN 3,751, and CDN 341 (2019 dollars) for 10%, 20%, 50%, and 100% market penetrations, respectively. These savings are considered insignificant per vehicle.

This study concludes that the overall benefits of using NG-WBT for the trucking industry significantly surpass the cost by the agency to maintain pavement serviceability.

Summary and Preliminary Findings

Life cycle cost analysis was performed to assess the economic impact of NG-WBT usage in New Brunswick, Canada. The procedure combines 3D finite-element models to calculate critical pavement responses, WIM data to determine traffic characteristics, regression analysis to compute critical pavement responses for any axle load, transfer functions to predict pavement damage, and empirical equations to estimate IRI progression.

From the structural evaluation under the specific conditions in this study, NG-WBT (445/50R22.5) resulted in pavement critical responses between 3 and 9 $\mu\varepsilon$ greater than DTA (275/80R22.5). Calculated pavement responses include tensile strain at the bottom of the AC and vertical shear strain in the AC. However, the difference was negligible for the vertical strain on the subgrade.

For an economic evaluation, the LCCA, which accounted for fuel savings and greater hauling capacity, resulted in cost savings when NG-WBT is used. Two scenarios were considered: (1) Case A, in which maintenance was performed at specific intervals regardless of IRI value, and (2) Case B, in which the IRI threshold triggers maintenance. In both scenarios, there were significant savings in trucking fuel costs.

The agency cost to maintain the pavement used by NG-WBT is expected to be between CDN 7,703 to CDN 8,840 (2019 dollars) for 10% and 20% of all tandem axles using NG-WBT per one kilometer for a 60-year analysis period. The annual worth of such a cost would be CDN 298 and CDN 342 (2019 dollars), respectively. In contrast, the fuel savings per truck-km is expected to be between CDN 31,161 and CDN 57,134 (2019 dollars) for 10% and 20% of all tandem axles using NG-WBT per one kilometer for the same analysis period. The annual worth of such savings per kilometer would be CDN 1,100 and CDN 2,172 (2019 dollars), respectively. In addition, the trucks would save annually CDN 0.042 and 0.107 per ton transporting one kilometer when NG-WBT market penetration is 10% and 20%, respectively. If the average truck loading is 40 t, the annual savings are CDN 1.68 and CDN 4.28 for 10% and 20% penetration, respectively. Maintaining a low IRI on the road would also benefit passenger vehicles, which make up most users.

In general, using NG-WBTs when maintaining pavement conditions at the same level as when only DTAs are used requires additional agency investment, which appears justified given the significant fuel savings by trucks.

Data Availability Statement

Some or all of the data, models, or code generated or used during the study are proprietary or confidential in nature and may only be provided with restrictions. Some of the data provided by the New Brunswick Department of transportation are confidential. Truck tire loadings were obtained from the tire manufacturer and are classified as proprietary.

Acknowledgments

The authors acknowledge the financial support provided by the New Brunswick Department of Transportation. This work used the Extreme Science and Engineering Discovery Environment (XSEDE) at the San Diego Supercomputer Center, which is supported by National Science Foundation Grant No. ACI-1548562. This project was conducted in cooperation with the Illinois Center for Transportation. The contents of this paper reflect the view of the authors, who are responsible for the facts and the accuracy of the data presented herein. The contents do not necessarily reflect the official views or policies of the Illinois Center for Transportation or the New Brunswick Department of Transportation. This paper does not constitute a standard, specification, or regulation.

References

AASHTO. 2008. *Mechanistic-empirical pavement design guide: A manual of practice*. Washington, DC: AASHTO.

Al-Qadi, I. L., and M. A. Elseifi. 2007. “New generation of wide-base tires: Impact on trucking operations, environment, and pavements.” *Transp. Res. Rec.* 2008 (1): 100–109. https://doi.org/10.3141/2008-13.

Al-Qadi, I. L., J. A. Hernandez, A. Gamez, M. Ziyadi, O. E. Gungor, and S. Kang. 2018. “Impact of wide-base tires on pavements: A national study.” *Transp. Res. Rec.* 2672 (40): 186–196. https://doi.org/10.1177/0361198118757969.

Al-Qadi, I. L., A. Loulizi, I. Janajreh, and T. E. Freeman. 2002. “Pavement response to dual tires and new wide-base tires at same tire pressure.” *Transp. Res. Rec.* 1806 (1): 38–47. https://doi.org/10.3141/1806-05.

Al-Qadi, I. L., I. Said, J. Hernandez, and S. Kang. 2017. *Impact and life cycle assessment of new-generation wide-base tires in New Brunswick, Canada*. Rantoul, IL: Illinois Center for Transportation.

Al-Qadi, I. L., R. Yang, S. Kang, H. Ozer, E. Ferrebee, J. R. Roesler, A. Salinas, J. Meijer, W. R. Vavrik, and S. L. Gillen. 2015. “Scenarios developed for improved sustainability of Illinois Tollway: Life-cycle assessment approach.” *Transp. Res. Rec.* 2523 (1): 11–18. https://doi.org/10.3141/2523-02.

Al-Qadi, I. L., and P. J. Yoo. 2007. “Effect of surface tangential contact stresses on flexible pavement response.” *J. Assoc. Asphalt Paving Tech- nol.* 76 (8): 663–692.

Austin, D. 2015. *Pricing freight transport to account for external costs*. Washington, DC: Congressional Budget Office.

Chatti, K., and I. Zaabar. 2012. *Estimating the effects of pavement con- dition on vehicle operating costs*. NCHRP Rep. 720. Washington, DC: Transportation Research Board.

Fakhri, M., and A. R. Ghanizadeh. 2014. “Modelling of 3D response pulse at the bottom of asphalt layer using a novel function and artificial neural network.” *Int. J. Pavement Eng.* 15 (8): 671–688. https://doi.org/10.1080/10298436.2013.851791.

Hernandez, J. A., I. Al-Qadi, and M. De Beer. 2013. “Impact of tire loading and tire pressure on measured 3D contact stresses.” In *Airfield and high- way pavement 2013: Sustainable and efficient pavements*, 551–560. Reston, VA: ASCE.

Hernandez, J. A., A. Gamez, and I. L. Al-Qadi. 2016. “Effect of wide- base tires on nationwide flexible pavement systems: Numerical mod- eling.” *Transp. Res. Rec.* 2590 (1): 104–112. https://doi.org/10.3141/2590-12.

Holt, A., S. Sullivan, and D. K. Hein. 2011. “Life cycle cost analysis of municipal pavements in southern and Eastern Ontario.” In *Transporta- tion successes: let’s build on them. Congress et Exhibition de l’Asso- ciation des Transports du Canada. Les Success en Transports: Une Tremplin vers l’Avenir*. Washington, DC: Transportation Research Board.

Kang, S., I. L. Al-Qadi, H. Ozer, M. Ziyadi, and J. T. Harvey. 2019. “Environmental and economic impact of using new-generation wide- base tires.” *Int. J. Life Cycle Assess.* 24 (4): 753–766. https://doi.org/10.1007/s11367-018-1480-6.

Kerali, H. G., J. B. Odoki, and E. E. Stannard. 2000. “Overview of HDM-4.” In Vol. 1 of *The highway development and management series*. Washington, DC: World Bank.

Okte, E., I. L. Al-Qadi, and H. Ozer. 2019. “Effects of pavement condition on LCCA user costs.” *Transp. Res. Rec.* 2673 (5): 339–350. https://doi.org/10.1177/0361198119836776.

Said, I. M., J. Hernandez, S. Kang, and I. L. Al-Qadi. 2020. “Structural and environmental impact of new-generation wide-base tires in New Bruns- wick, Canada.” *Road Mater. Pavement Des.* 21 (7): 1968–1984. https:// doi.org/10.1080/14680629.2019.1590219.

Tutumluer, E. 2009. “State of the art: Anisotropic characterization of unbound aggregate layers in flexible pavements.” In *Proc., Pavements and Materials: Modeling, Testing, and Performance*, 1–16. Reston, VA: ASCE.

Wang, D., J. R. Roesler, and D. Z. Guo. 2009. “Analytical approach to predicting temperature fields in multilayered pavement systems.” *J. Eng. Mech.* 135 (4): 334–344. https://doi.org/10.1061/(ASCE)0733-9399(2009)135%3A4(334).

Yoo, P., and I. Al-Qadi. 2007. “Effect of transient dynamic loading on flex- ible pavements.” *Transp. Res. Rec.* 1990 (1): 129–140. https://doi.org/10.3141/1990-15.

Yoo, P. J., and I. L. Al-Qadi. 2008. “The truth and myth of fatigue cracking potential in hot-mix asphalt: Numerical analysis and validation.” In Vol. 77 of *Proc., Asphalt Paving Technology*, 549–590. Lino Lakes, MN: Association of Asphalt Paving Technologists.

Yoo, P. J., I. L. Al-Qadi, M. A. Elseifi, and I. Janajreh. 2006. “Flexible pavement responses to different loading amplitudes considering layer interface condition and lateral shear forces.” *Int. J. Pavement Eng.* 7 (1): 73–86. https://doi.org/10.1080/10298430500516074.

Ziyadi, M., H. Ozer, S. Kang, and I. L. Al-Qadi. 2018. “Vehicle energy consumption and an environmental impact calculation model for the transportation infrastructure systems.” *J. Cleaner Prod.* 174 (Feb): 424–436. https://doi.org/10.1016/j.jclepro.2017.10.292.

Figures

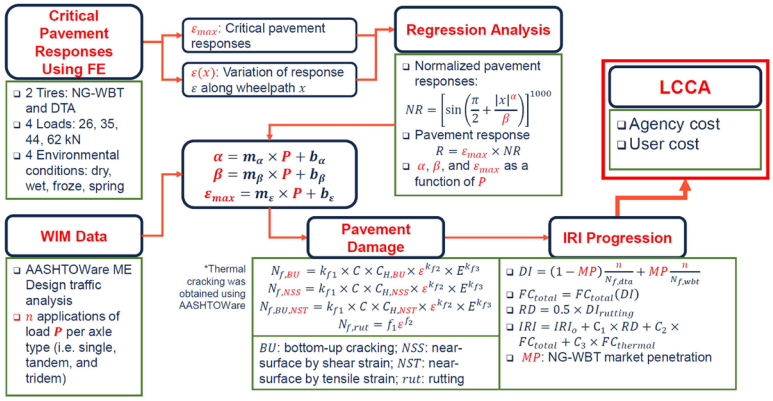

Fig. 1. Summary of procedure to perform LCCA.

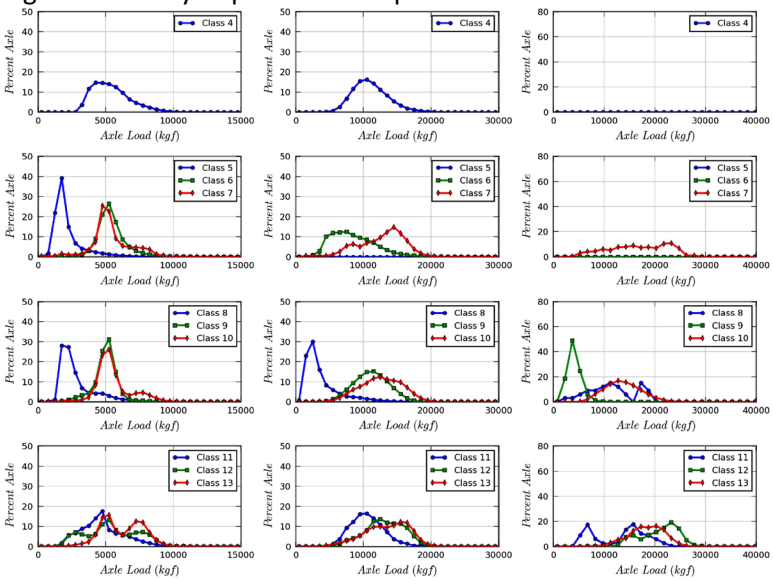

Fig. 2. Average normalized axle load spectra.

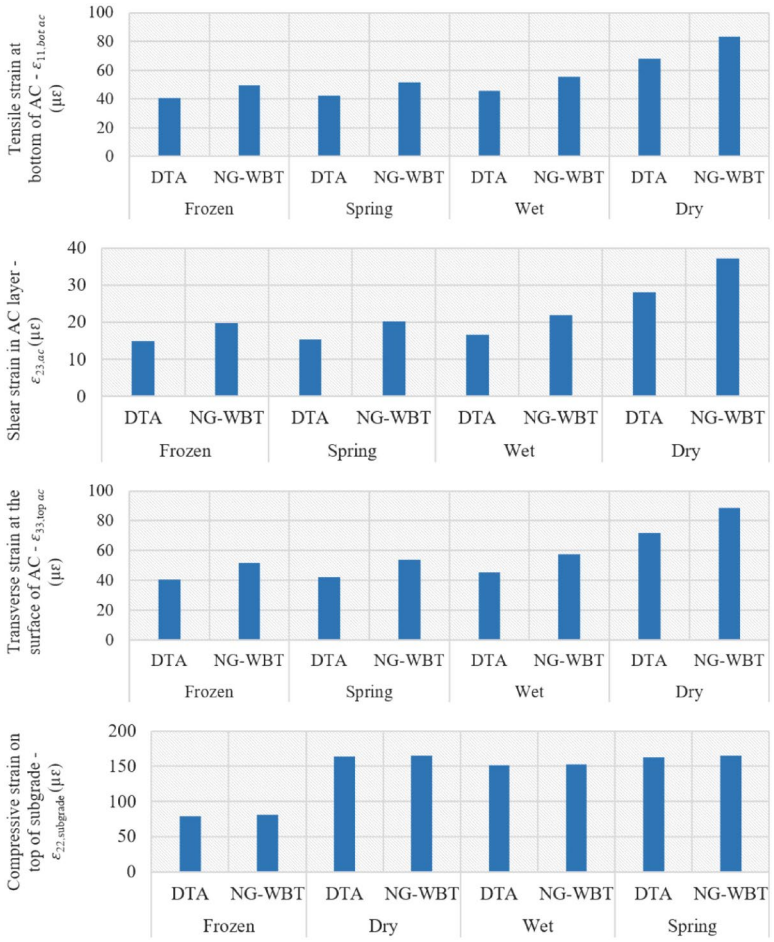

Fig. 3. Comparison of critical pavement responses between DTA and NG-WBT at 36 kN.

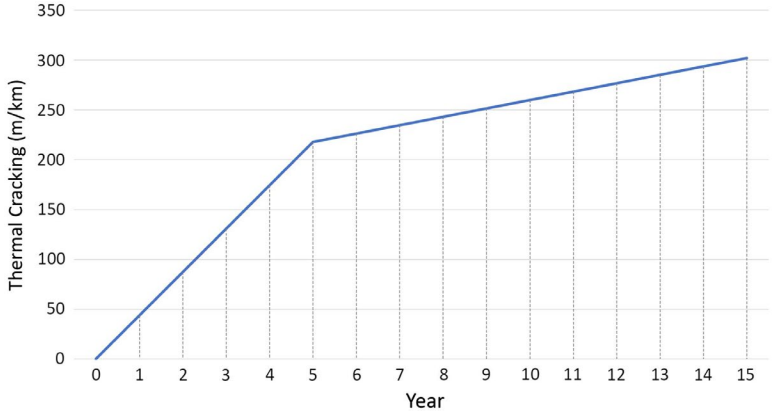

Fig. 4. Area of thermal cracking for a duration of 15 years.

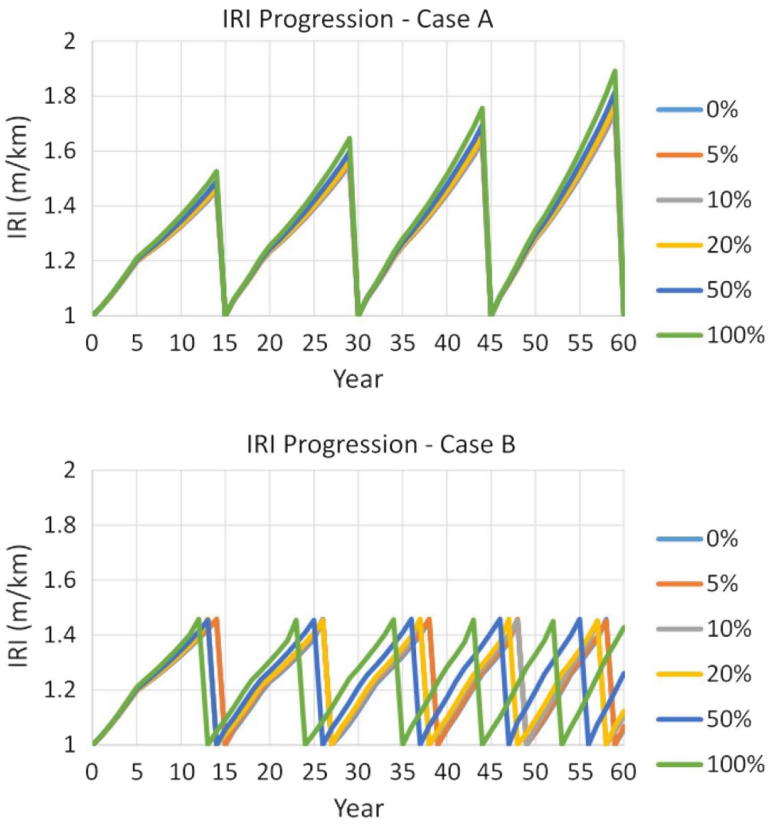

Fig. 5. IRI progressions for cases A and B considering various market penetrations.

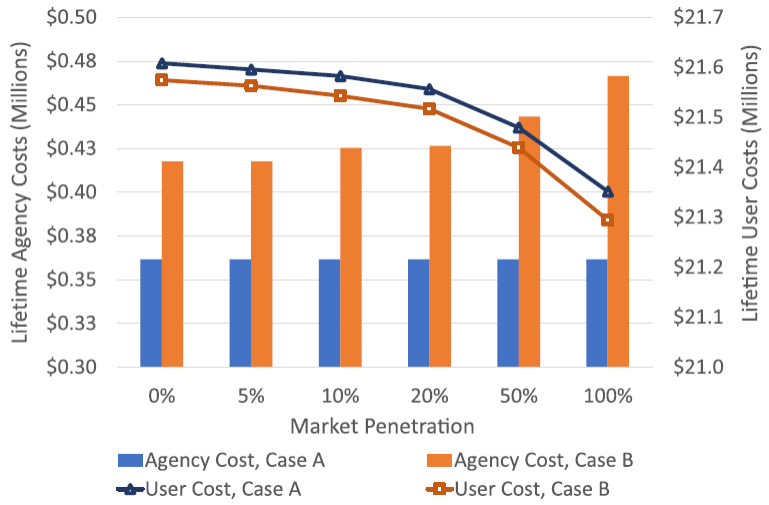

Fig. 6. Market penetration versus lifetime costs (present cost) in CDN per km.